Roll control of a Small Amateur Rocket

Technical Report · May 2009

CITATIONS
0

READS
368

1 author:

Craig Strudwicke
Transport for NSW
3 PUBLICATIONS **1** CITATION

SEE PROFILE

Roll control of a Small Amateur Rocket

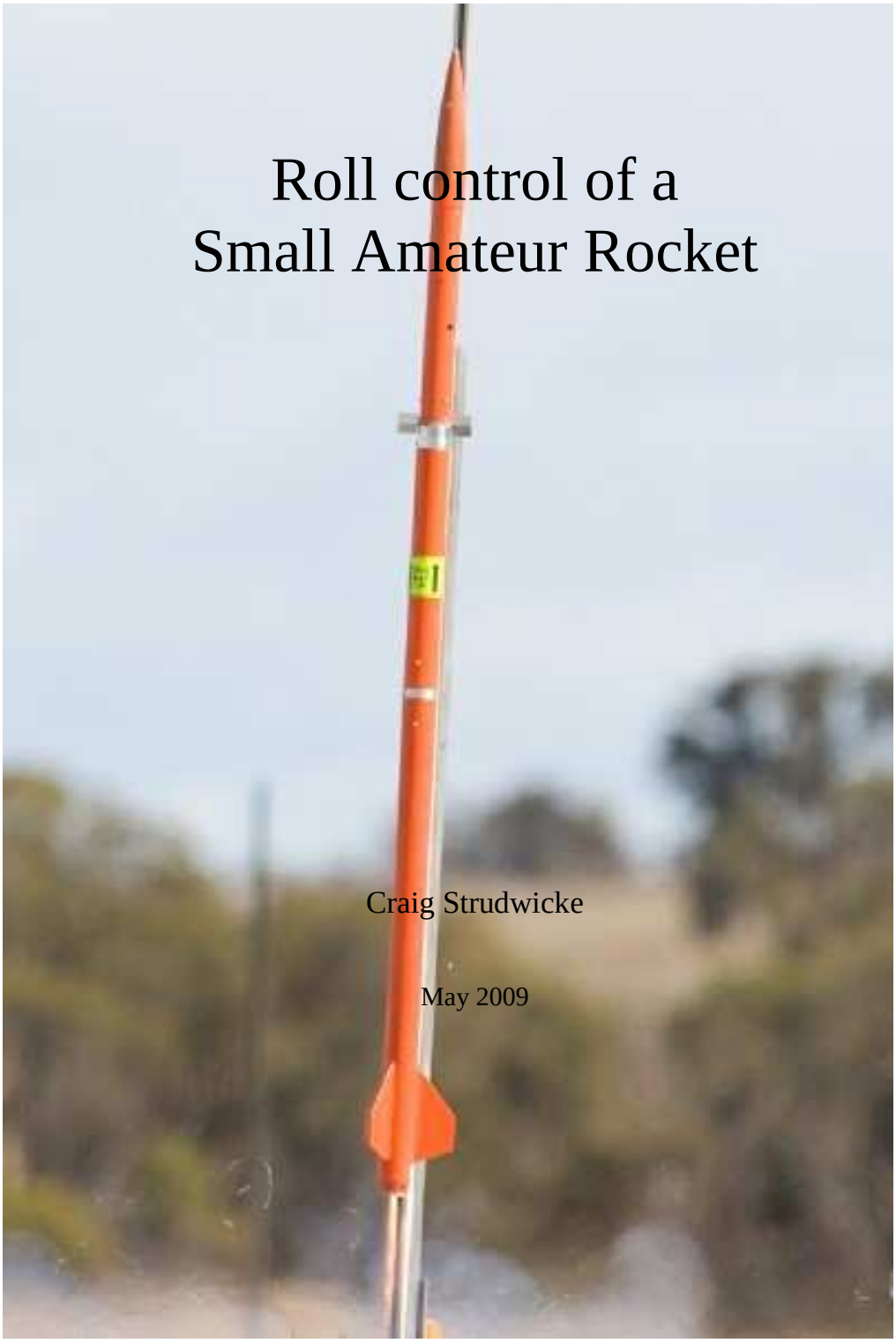

Craig Strudwicke

May 2009

E.R.G.
"Ad terra per aspera"

Abstract

For a number of reasons, the ability to control roll rate &/or roll angle of a rocket is an attractive idea. Some examples are for image gathering and antennae positioning. Another motivation is so that attitude measurements can be made that can easily be processed.
This paper discusses a sensor system consisting of a tri-axial magnetometer and a rate gyro as the sensing elements, with a pair of small fins driven in differential mode as the roll torque actuator.
A small rocket was flown a number of times with this system in place and shown to work well.

Acknowledgments

A great deal of assistance has been provided by Paul Kelly during this work, namely in construction, assistance with launch testing and as a technical sounding board.

Andrew Burns has assisted providing aerodynamic modelling advice and formulae for the small fin actuators used.

Sampo Niskanen has also provided valuable assistance with his review of the data and results.

Contents

List of Figures

List of Tables

1 System concept

The idea is to provide a roll controller that can maintain an absolute value WRT the earth/launch datum. To do this, some absolute sensing system is required. One such sensor system is a tri-axial magnetometer, which returns 3 orthogonal magnetic field readings enabling the calculation of a field vector. When evaluated in the XY (horizontal) plane, the magnetic heading/roll angle can be evaluated.
The error between the desired roll angle and actual is used to generate a command to the servo actuator that drives a pair of aerodynamic surfaces differentially to generate a restoring roll torque. The following block diagram gives an overview of this system architecture.

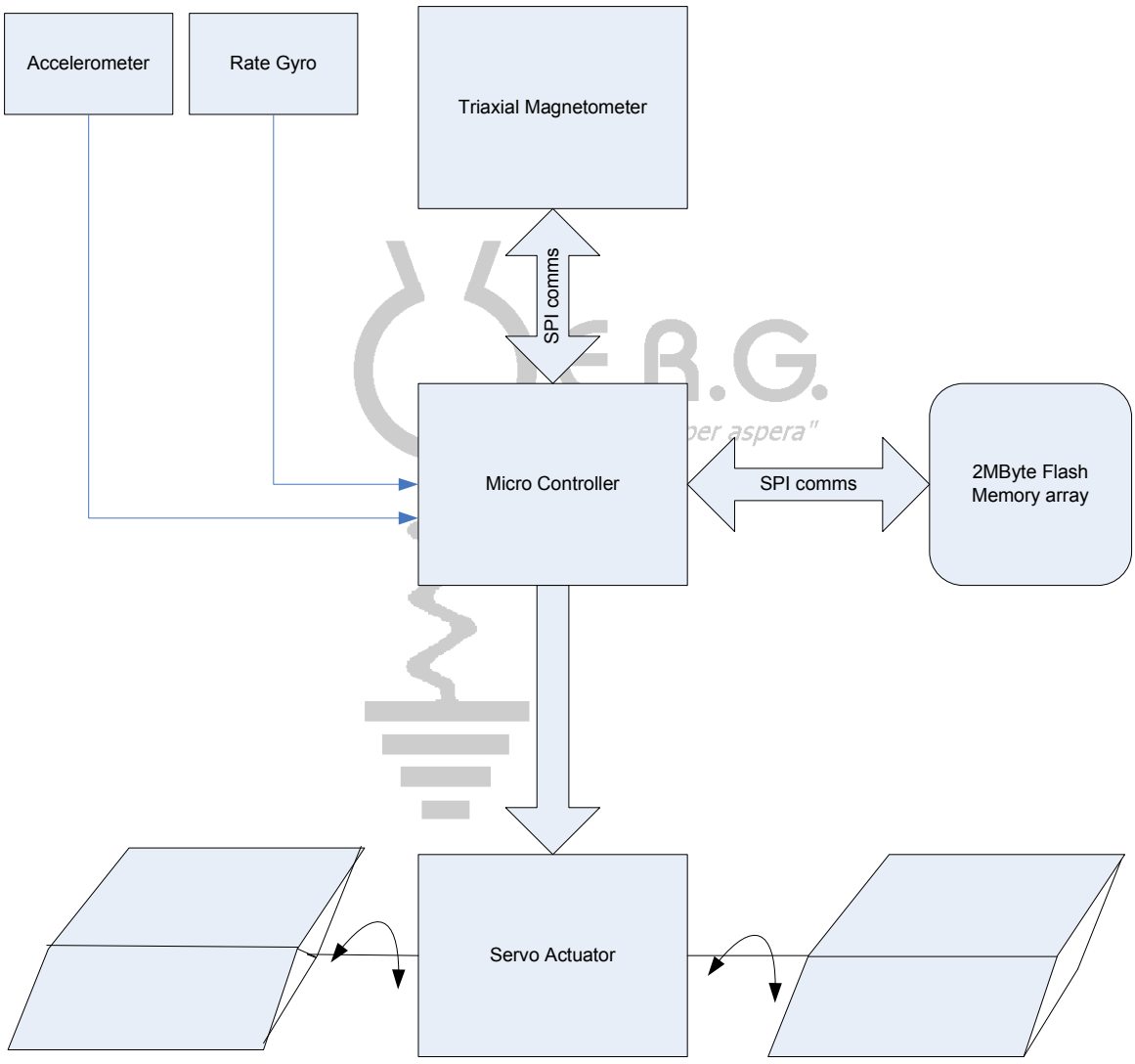

Figure 1 – System Block diagram

2 Roll Control Actuator

An actuator is required to provide a correcting roll torque to control the roll angle and roll rate of a rocket.
The decision was made that the most practical and efficient manner for this to be done at this time and in the vehicles currently being flown was to use aerodynamic surfaces ie fins.

2.1 Aerodynamic Surfaces

The following performance requirements were set out to provide some design constraints for these fins and the actuator to drive them.

- Desired closed loop natural period - 1.0Hz
- Desired closed loop damping factor – 0.7
- Actuator resolution @ surface – 0.1° (angle of attack)

Some relevant vehicle parameters are :

- Burnout Mass : 3.5kg
- Diameter : 65mm
- Estimated Rotational Inertia : 0.001575 kgm^2
- Range of airspeed : up to 450m/s

The following formulae are used in a spreadsheet model to simulate the performance of the fin actuator pair.

$$C_L = C_{L_\alpha} \cdot \alpha \qquad \text{eqn 2.1}$$

Where:

C_{L_α} = lift slope & is 2.5 for this fin shape & size[1]
C_L = Lift coefficient (non-dimensional)
α = Control surface angle of attack in radians

Then:

$$L = \frac{1}{2}\rho V^2 C_L S \qquad \text{eqn 2.2}$$

Where:

L = Control surface lift force (N)
ρ = Air density (kgm-^{3})
V = Air velocity (ms^{-1})
S = Fin area (m^2)

And the moment acting on the fin can be found using this equation (assuming the fin is supported at the half chord location).

$$M_\theta = L \cdot \frac{1}{2} c \qquad \text{eqn 2.3}$$

Where:

$M_\theta =$ Moment at half chord (Nm)
$c =$ Fin chord length (m) (distance from leading edge to trailing edge)

Now calculating roll torque or torque about the Φ axis.

$$M_\phi = 2L \cdot r \qquad \text{eqn 2.4}$$

Where :

$M_\phi =$ Roll torque generated (Nm)
r = radius of action ie distance from roll axis to centre of fin (m)

Substituting 2.1 & 2.2 into 2.4 yields :

$$M_\phi = 2r \cdot \rho V^2 \cdot C_{L_\alpha} \cdot \alpha \cdot S \qquad \text{eqn 2.5}$$

A control parameter referred to later in this paper is G_a or aerodynamic gain, is calculated :

$$G_a = 2r \cdot \rho V^2 \cdot C_{L_\alpha} \cdot S \qquad \text{eqn 2.6a}$$

or

$$G_a = \frac{M_\phi}{\alpha} \qquad \text{eqn 2.6}$$

G_a or aerodynamic gain represents the torque capacity of the fin pair acting in differential mode for a unity displacement.

Now to generate the functions to be used to calculate the gain schedules for the controller.

Equation of motion in standard form for a 2nd order system is :

$$\ddot{\phi} + 2\zeta\dot{\phi}\omega_n + \omega_n{}^2\phi = 0 \qquad \text{eqn 2.7}$$

Where :

$\ddot{\phi}$ - angular acceleration, $\dot{\phi}$ - angular velocity and $\ddot{\phi}$ - angular displacement.
ζ - damping factor (dimensionless)
ω_n - natural frequency (Hz)

Specific equation of motion for the vehicle including control torque :

$$J\ddot{\phi} + d\dot{\phi} + k\phi = \Delta\theta.G_a \qquad \text{eqn 2.8}$$

Where :

J – rotational inertia (kgm^2)

d – rotational damping (Nm s/rad)
$\Delta\theta$ - fin delta theta ie control action
G_a - aerodynamic gain (Nm/rad)

The control term is made up of three components when implementing a PID control algorithm:

$$\Delta\theta = Kp(\phi_{ref} - \phi) + Kd(\dot{\phi}_{ref} - \dot{\phi}) + Ki\int(\phi_{ref} - \phi)dt \qquad \text{eqn 2.9}$$

Initially it is intended that the controller will only be PD with no integral component since an integral term reduces robustness and degrades recovery from perturbations.

Assuming a reference velocity and angle of 0, substituting eqn 2.3 into eqn 2.2 yields :

$$J\ddot{\phi} + (d + KdG_a)\dot{\phi} + (k + KpG_a)\phi = 0 \qquad \text{eqn 2.10}$$

Now changing to the standard form for a 2nd order system :

$$\ddot{\phi} + (d + KdG_a)\dot{\phi}/J + (k + KpG_a)\phi/J = 0 \qquad \text{eqn 2.11}$$

Therefore, the following equations are generated from eqn 2.11 being in the standard form as per eqn 2.7.

$$\frac{d + K_d G_a}{J} = 2\zeta\omega_n$$

$$K_d = \frac{2J\zeta\omega_n - d}{G_a} \qquad \text{eqn 2.12}$$

$$\frac{k + K_p G_a}{J} = \omega_n^2$$

$$K_p = \frac{J\omega_n^2 - k}{G_a} \qquad \text{eqn 2.13}$$

Note both K_d & K_p are inversely proportional to G_a. The gain schedule is an important aspect of the control system since the actuator roll torque capacity as a function of airspeed *(G_a)* is highly variable over the range of velocity the vehicle will be operating in due to it being proportional to V^2.

Note that both k & d would need to be determined by in-flight testing and are entirely determined by each vehicles specific aerodynamic characteristics. To greatly simplify the generation of these gain schedules, both k & d have been assumed to be zero in this instance[1].

Having this model allowed some design iterations to be performed and a fin 'size' and profile was decided upon. Note that the whole actuator is rotated since it is very likely that it will be operated at supersonic speeds.

[1] An assumption of k=0 is entirely reasonable unless there is a passive roll control device fitted. Assuming d=0 has been done simply because the method to measure this does not exist at this time.

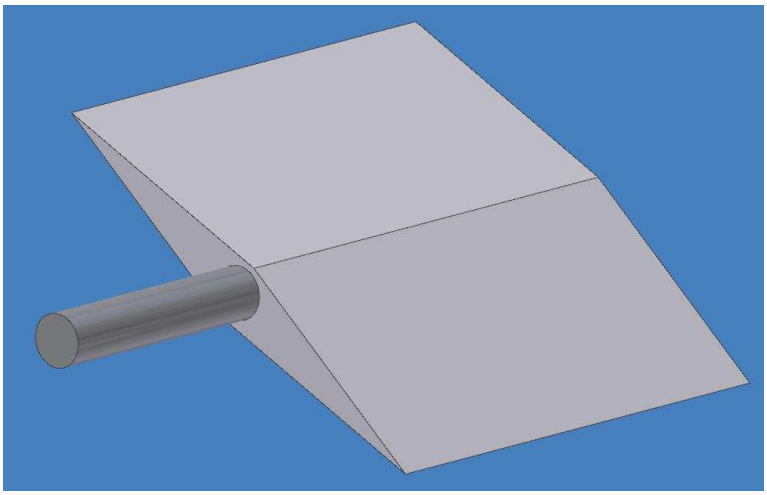

Figure 2 – Chosen fin shape

Fin parameters :

- Chord : 0.038 m
- Length : 0.038 m
- Thickness : 0.005 m
- Area : 0.001444 m^2
- Lift Slope : 2.5

The expected characteristics of this fin pair & the gain schedule required to implement the desired dynamics is shown in the following chart.

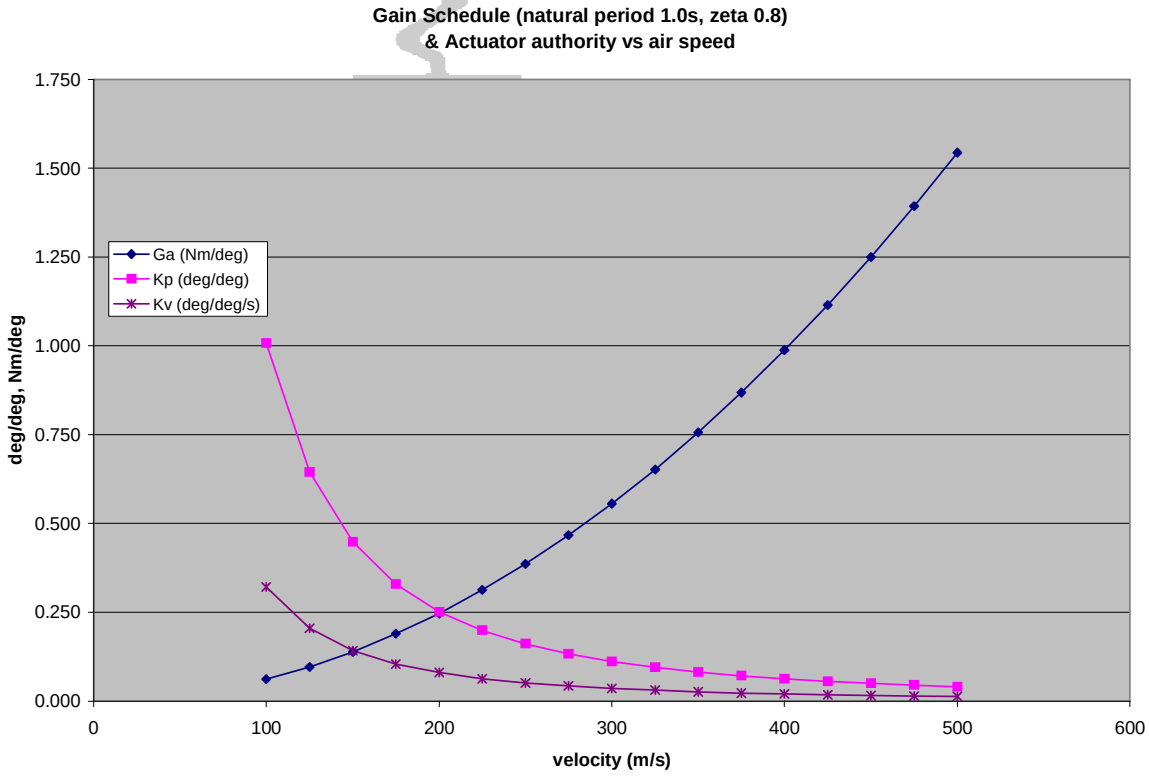

Figure 3 – Gain schedule & Actuator Authority as a function of velocity

As the above chart shows, a large variation in Ga is observed over the potential operating range of the vehicle, infact a 20x increase from 100m/s to 450m/s. This is why the gain schedule is required to ensure consistent closed loop performance as velocity changes.

2.2 Servo Actuator implementation

A single actuator is used to drive two fins in differential mode. Due to the small diameter of the vehicle (60mm) a special purpose housing and mechanism was manufactured to implement this arrangement.

Figure 4 – RC servo mounting/actuator housing

The RC-Servo used in this instance was an NES-331 Micro servo with the following parameters :

- Torque capacity : 3.2kgcm (0.314Nm)
- Dimensions : 30 x 13 x 28.5mm
- Mass : 18g
- Speed : 0.24s / 60deg

The servo actuator is connected to the fin shaft via a modified servo horn, a rigid link and a bell crank. This linkage system drives the pair of fins in a differential manner.

A purpose built 5V supply was made for the servo to run from, independent of the other circuitry. This was done to improve isolation from any large currents and associated electrical noise.

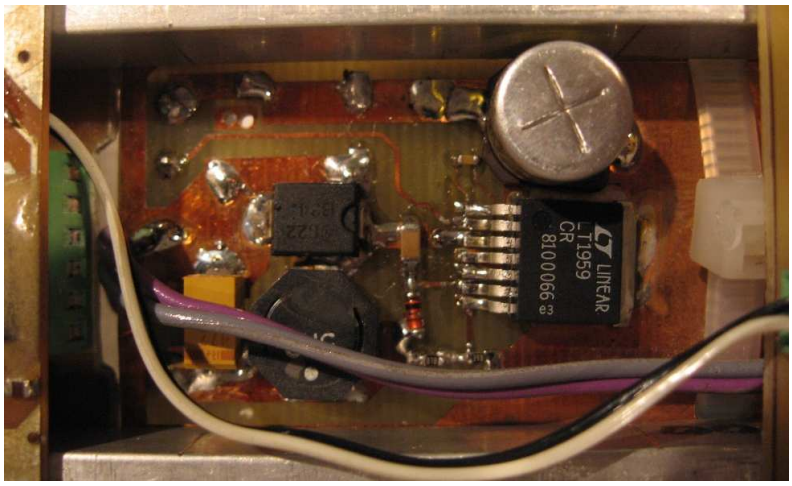

Figure 5 – Servo actuator 5V SMPS rated at 4A

A relatively oversized Lithium Polymer battery was installed to provide all the electrical power for the test module. It was rated at 1700mAh with a nominal voltage of 7.2V, although it did not drop below 7.9V after a whole day of testing and flights after being charged to 8.4V initially.

Figure 6 – Lithium Polymer battery used to supply all of the modules power

2.3 Actuator Calibration

A simple calibration process was carried out to determine the transfer function between commanded servo period and fin actuation. A laser engraved scale was created along with a special pointer designed to slip over the chosen fin section.

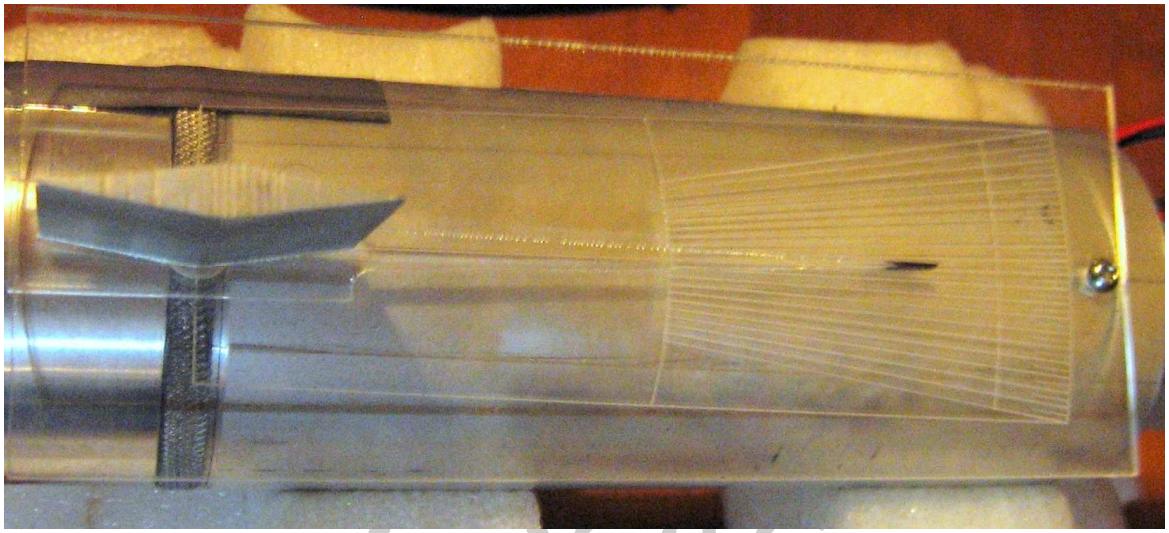

Figure 7 – Servo actuator calibration apparatus

The actuator was commanded to move to various positions and readings were taken from this scale by eye with an uncertainty of $\approx 0.2°$ with the uncertainty of the laser engraving to be $\leq 0.1°$.

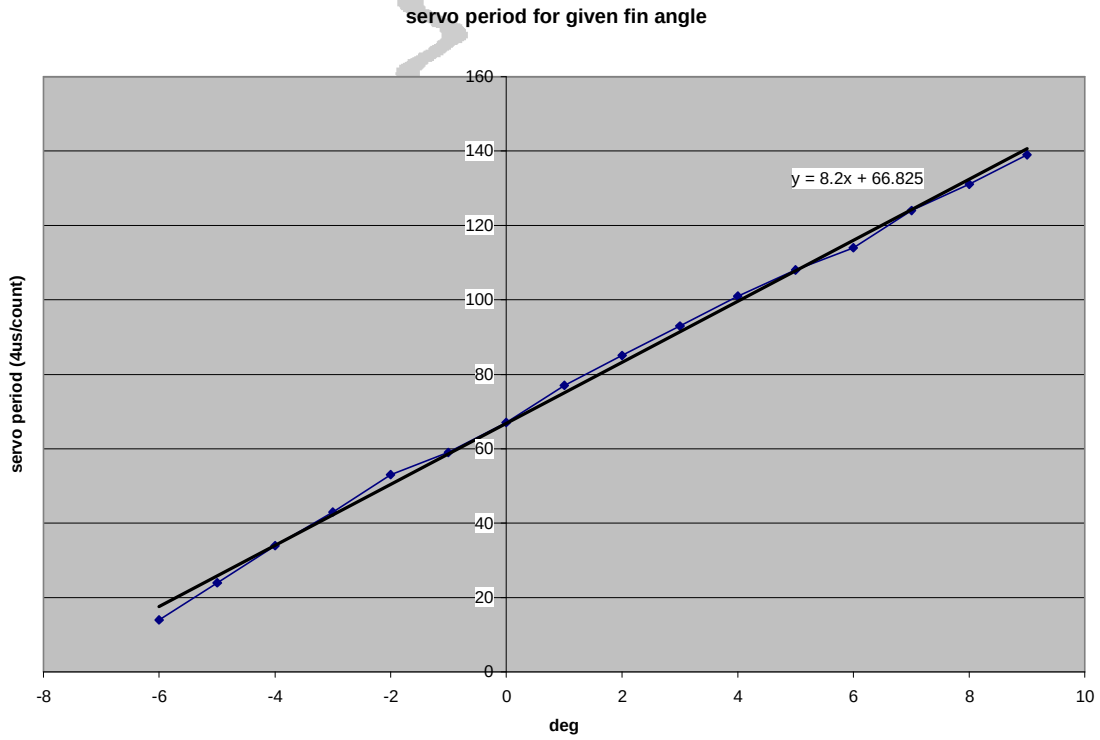

Figure 8 – Servo actuator characterisation chart

The transfer function for this actuator assembly is approximated well by a linear function :

$\theta_a = \theta c \times m_a + b_a$ (as shown on chart)

The largest error using this transfer function is 4% FS at the extreme negative actuation.

3 Controller Implementation

3.1 Hardware

As shown in figure 1, section 1, a microcontroller is used to implement the Roll Control and other functions.
The microcontroller used in this prototype is a Microchip PC18LF2520. It is run at 20MHz and is able to read all sensors, perform ATAN2 function, execute the control algorithm, write to the flash memory with a little time to spare in a 40Hz loop.

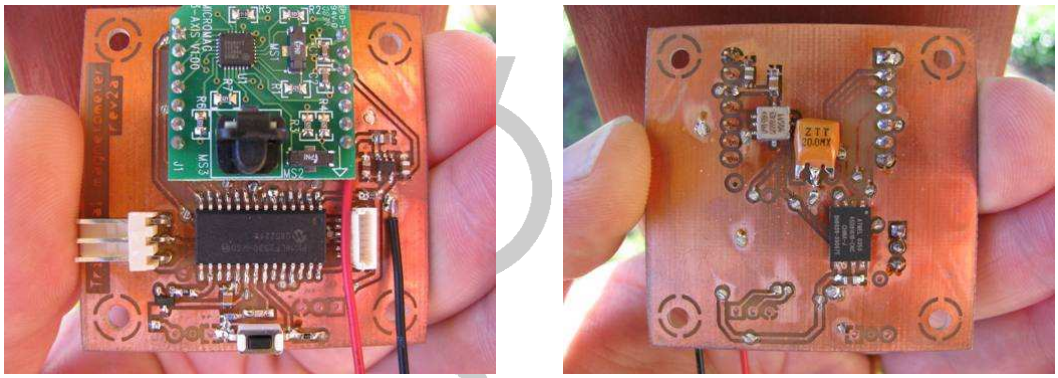

Figure 9 – Controller circuit board

The following I/O is utilised :

Signal Name	Type	Units	Range	Description
SO	Digital input			Slave Out
SI	Digital output			Slave in
Ready	Digital Input			Magnetometer Status
Clk	Digital out			SPI clock
CS1	Digital out			Magnetometer CS
CS1	Digital out			Memory Chip CS
AN0	Analog In	V	0 to 3.6	Rate gyro signal
AN1	Analog In	V	0 to 3.6	Acceleration signal
Tx	Digital Out			UART Output
Rx	Digital In			UART Input
ServoOut	Digital Out			Servo cmd
Status	Digital Out			Status LED
Arm	Digital Input			Arming Input

Table 1 – Micro controller I/O

3.1.1 Flight hardware assembly

All of the required components were mounted onto a robust chassis consisting of 10mm square section solid aluminium rails drilled and tapped for direct mounting of boards.

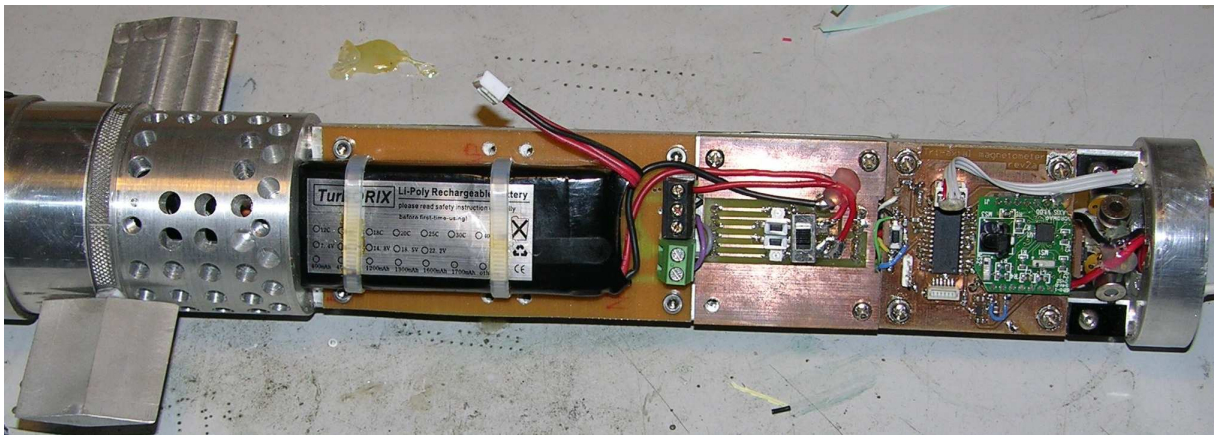

Figure 10 – Flight module topside

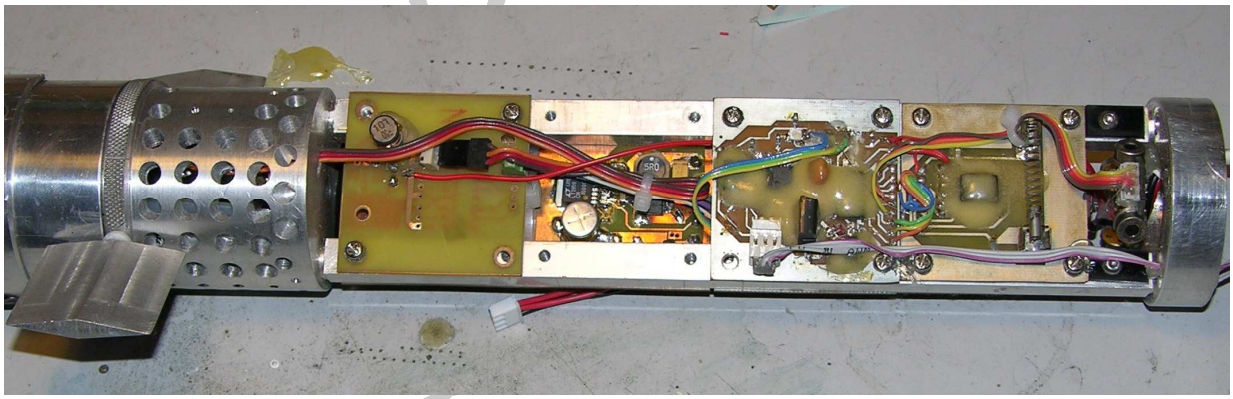

Figure 11 – Flight module backside

The serial ports of both the roll controller and the general purpose data logger were connected to the umbilical which was fed through to top bulkhead for easy access between flights hence reducing the vehicle turnaround time.

Figure 12 – Sensing elements

3.2 Software

The Control algorithm and other functions are implemented in the C programming language. The high level sequence of operation is best described by the following State Transition Diagram.

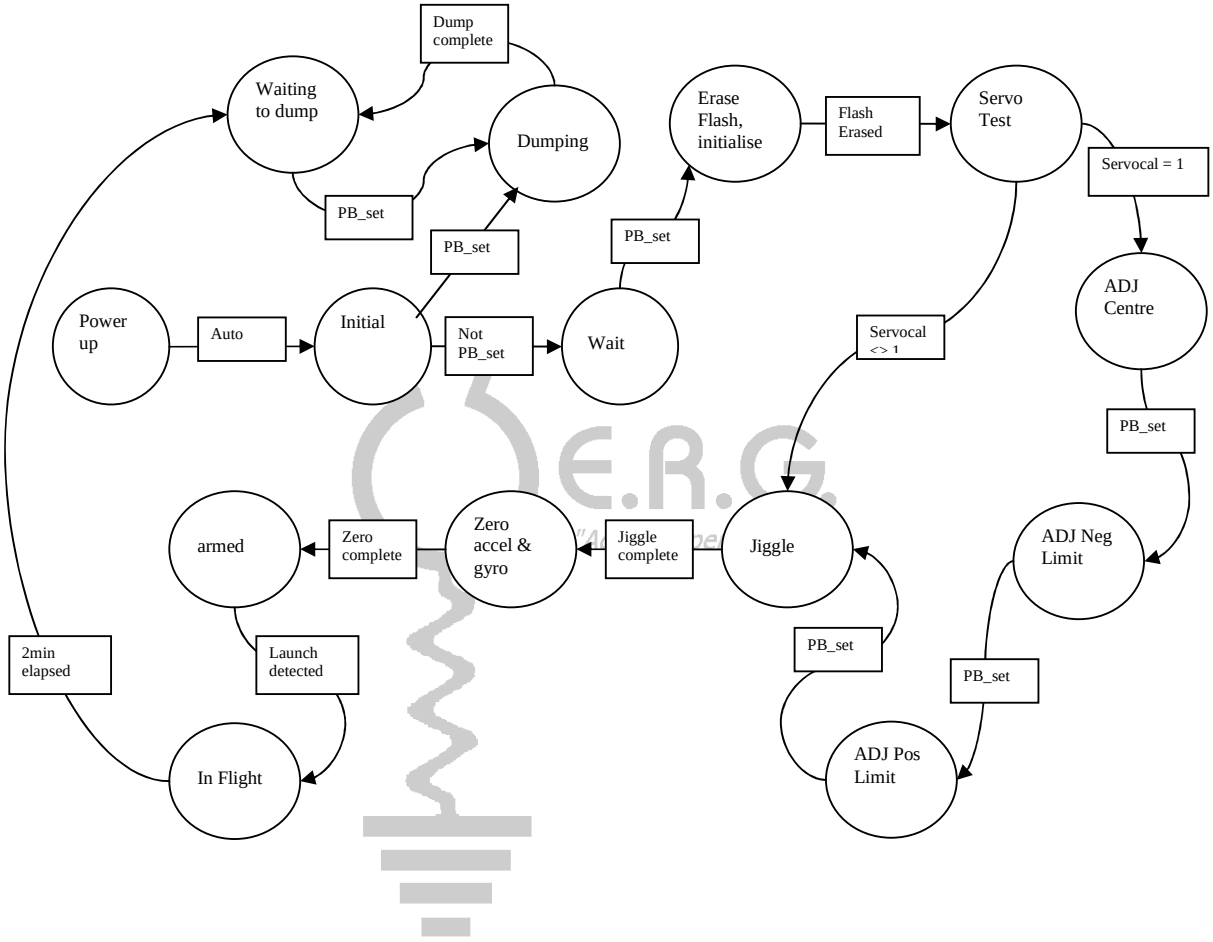

Figure 13 – State Transition diagram

PB_set refers to the digital input provided on board as a small push button. This is used in a number of places as the state transition trigger.

In most cases, the ***ServoCal*** Boolean will be set to false so that calibration/adjustment of the servo travel limits and centre position is bypassed.

The ***Launch Detected*** transition trigger is a 1G level sensed by the accelerometer.

3.2.1 Roll Control algorithm

The state described as ***In Flight*** is where all the actual roll control and associated functions are carried out.
This diagram describes the loop that is the ***In Flight*** state.

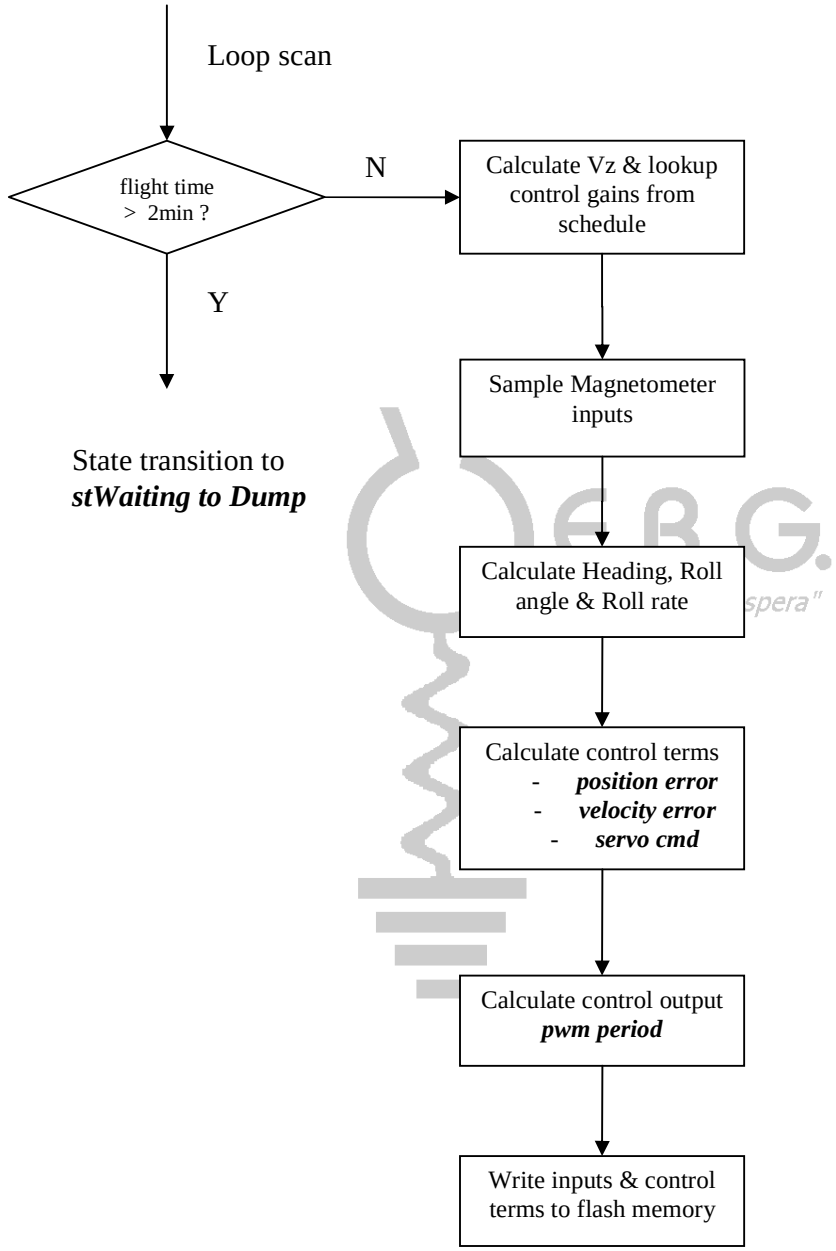

Figure 14 – 'In Flight' software process

This state is executed within a loop executed at 25ms intervals.

3.2.1.1 Calculation of terms

The Magnetometer provides three measurements, those being H_x, H_y, H_z representing magnetic field strength along X, Y & Z axes.
These readings are used to calculate the heading angle and subsequently the craft roll angle Θ.

This is calculated using :

$$\Theta = a\tan 2INT(H_x, H_y)$$

where atan2INT is a special implementation of the atan2 function using piecewise linear approximation and returns angle in 1/8th deg resolution. (insert reference to appendix)

The control terms are calculated as follows :

Position error term :

$$e_p = \Theta_{nom} - \Theta$$

Velocity error term :

$$e_v = \dot{\Theta}_{nom} - \dot{\Theta}$$

Control term :

$$\theta_d = k_p \times e_p + k_v \times e_v \qquad \text{(desired actuator angle)}$$

Control output :

$$pwm = \theta_d \times m_{act} + b_{act} \qquad \text{(units of counts for timer 2)}$$

3.2.2 Timing & PWM generation

Two hardware timers are used to implement the PWM signal and the control loop tick generator.

Timer0 is setup to timeout and generate an interrupt every 1ms and is used to increment a tick counter. This tick counter is used to control execution rate of the main loop and to measure flight time etc.

Timer2 is setup to count down at a rate of 250kHz or 4μs/count. It is loaded with a variable value to implement the PWM signal required of RC servo actuators. This is a pulse with duration from 1.0ms to 2.0ms every 20ms with a nominal 1.5ms centre position.

3.2.3 Serial Command Interface

A serial command interface was included so that parameters stored in EEPROM could be modified in the field. A summary of those commands follows :

command	description	parameter range	parameter size	Comments
rs	reset state machine	none		
sc	servo calibration	0, 1	1 byte	0 disables servo cal, 1 enables
kp	roll position loop gain scaling factor	0 to 16	1 byte	8 is unity, 0 disables position loop
kv	roll velocity loop gain scaling factor	0 to 16	1 byte	8 is unity, 0 disables velocity loop
fv	velocity feedback select	0 or 1	1 byte	0 : mag, 1: gyro
fp	position feedback select	0 or 1	1 byte	0: mag, 1: integrated gyro
df	dump logged flash data	none		
md	mode	0,1,2,3,4,5	1 byte	0 : flight mode, no debug
				1 : flight mode + debug
				2 : ground mode
				3 : ?
				4 : ?
				5 : ?
+	increment	NA		
-	decrement	NA		
?	command list	NA		
de	dump EEProm params	NA		
gs	get live servo period	NA		
ga	get live acceleration	NA		
gg	get live gyro rate	NA		
gx	get live mag X reading	NA		
gy	get live mag Y reading	NA		
gz	get live mag Z reading	NA		
sd	set current attitude and orientation as datum			
sa	set accel zero			
ss	set servo command			
sg	set gyro zero			

Table 2 – Serial command set

4 Flight testing

4.1 Test series 1 – May 2009

First time out testing, the vehicle was flown 5 times. Four of these flights were considered successful with one failure due to propulsion issues.

Typical flight profile :

Boost Acceleration : $75ms^{-2}$
V max : $125ms^{-1}$
Apogee : ≈ 1000m

Figure 15 – Launch vehicle 'This way up' prepped & ready

Roll controller settings :

Flight controller firmware revision : r2e

Gain Schedule for 1.0s closed loop period, damping factor of 0.8 :

Velocity (m/s)	Ga (Nm/deg)	Kp (deg/deg)	Kv (deg/deg/s)
50	0.015	4.028	1.026
75	0.035	1.790	0.456
100	0.062	1.007	0.256
125	0.096	0.644	0.164
150	0.139	0.448	0.114
175	0.189	0.329	0.084
200	0.247	0.252	0.064
225	0.313	0.199	0.051
250	0.386	0.161	0.041
275	0.467	0.133	0.034
300	0.556	0.112	0.028
325	0.652	0.095	0.024
350	0.756	0.082	0.021
375	0.868	0.072	0.018
400	0.988	0.063	0.016
425	1.115	0.056	0.014
450	1.250	0.050	0.013
475	1.393	0.045	0.011
500	1.544	0.040	0.010

Table 3 – Gain Schedule, testing May 29, 2009

4.1.1 Roll Controller Results

The following charts document the various parameters for each of these flights. Where suitable, results from multiple flights are shown on the one chart for comparative purposes.

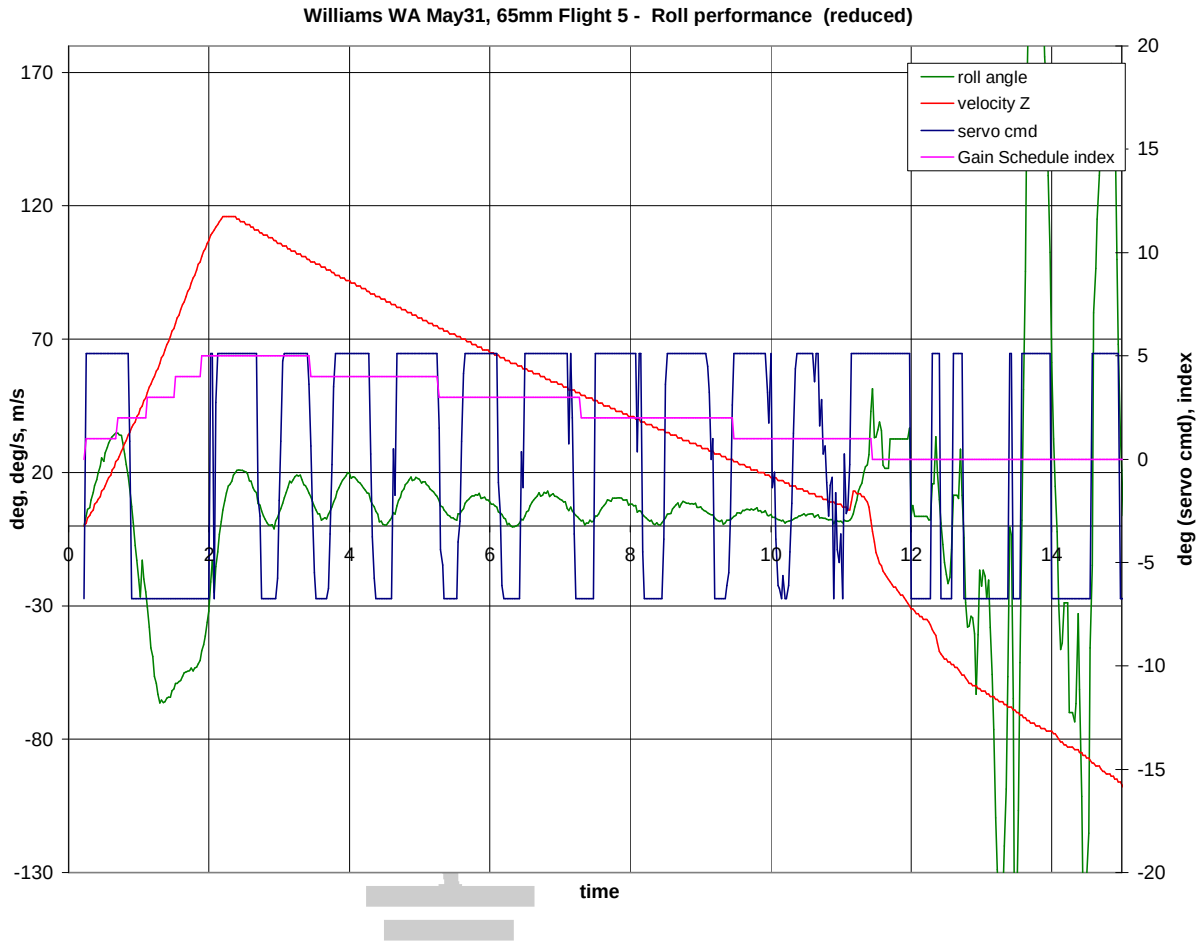

Figure 16 – Flight 5 roll angle performance

This chart is a good example of the typical performance for the 4 successful flights. It shows the servo command signal saturating badly and the roll angle oscillating significantly. The Gain Schedule index is shown to give some perspective on what is happening with the gains during the flight.

Even though the control action is not ideal, the roll angle is being controlled and held within 20deg of nominal for the majority of the flight.

Due to the asymmetry of the fin actuator travel and the saturating behaviour, there is a +ve bias to the roll angle.

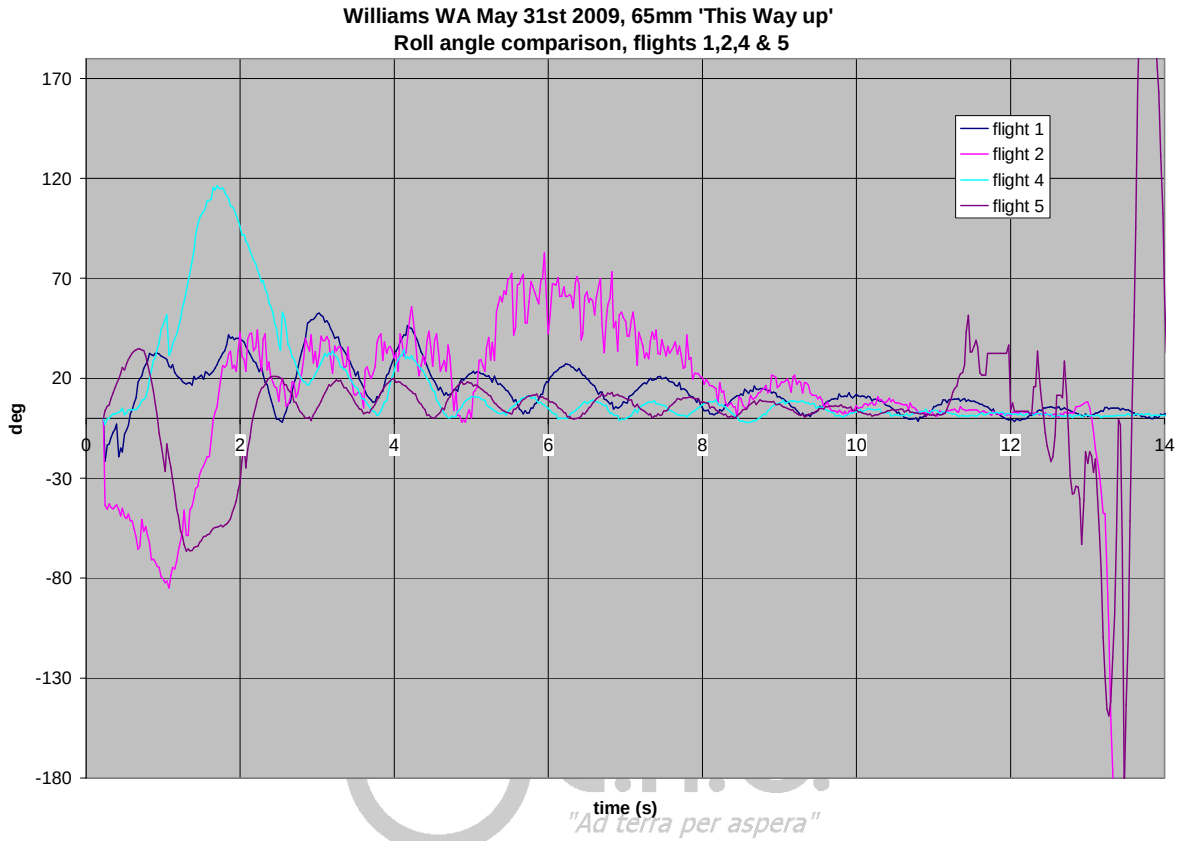

Figure 17 – Roll angle performance

As shown in the chart above, the roll angle typically had a large perturbation during the early boost phase which was brought back under reasonable control during the remainder of the flight up to the apogee recovery event. Also quite evident is the oscillatory characteristic of the roll angle. Estimated closed loop periods of 1.1s, 1.0s, 1.0s & 0.85s for flights 1,2,4 &5 respectively. These are quite close to the target period of 1.0s.

The high frequency components present in flight 2 could be due to slippage between the upper and lower sections of the airframe, which were coupled using a friction fit.

The very steep negative change in roll angle for flight 2 is troubling. The rate gyro signal and the magnetometer roll rate do not correspond well at this time. This comparison is best shown in Figure 18.
A large negative roll rate is reported by the magnetometer whilst the rate gyro signal is very small.

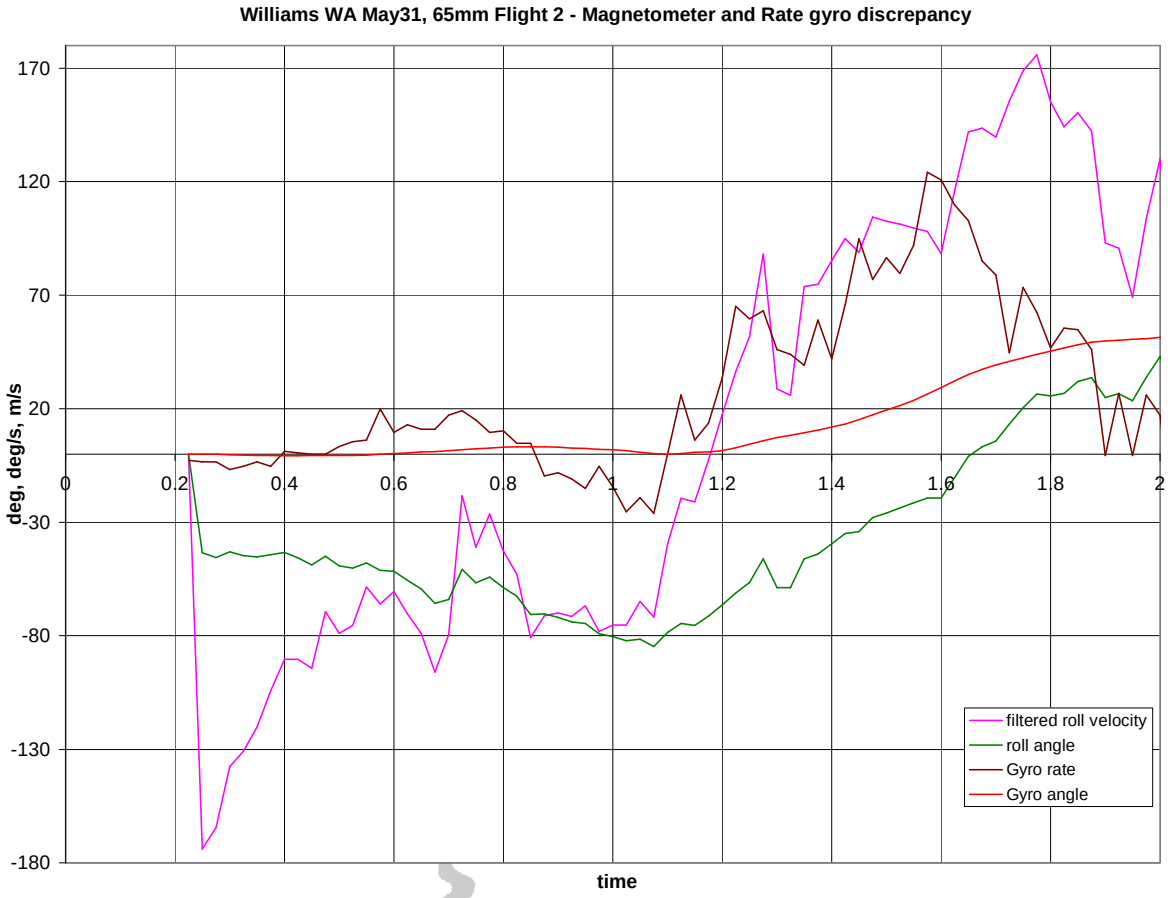

figure 18 – Rate gyro and magnetometer rate discrepancy

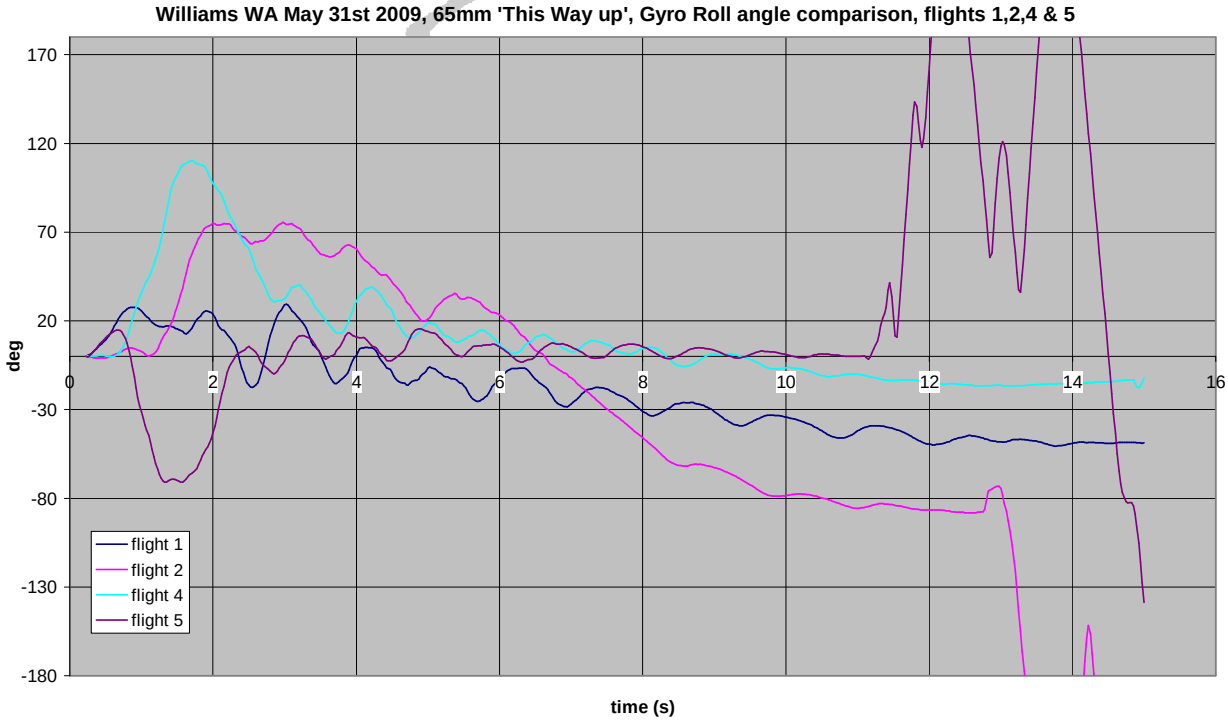

Figure 19 – Gyro angle comparison

This ‘gyro angle’ has been integrated from the rate gyro signal during the post processing of the data.

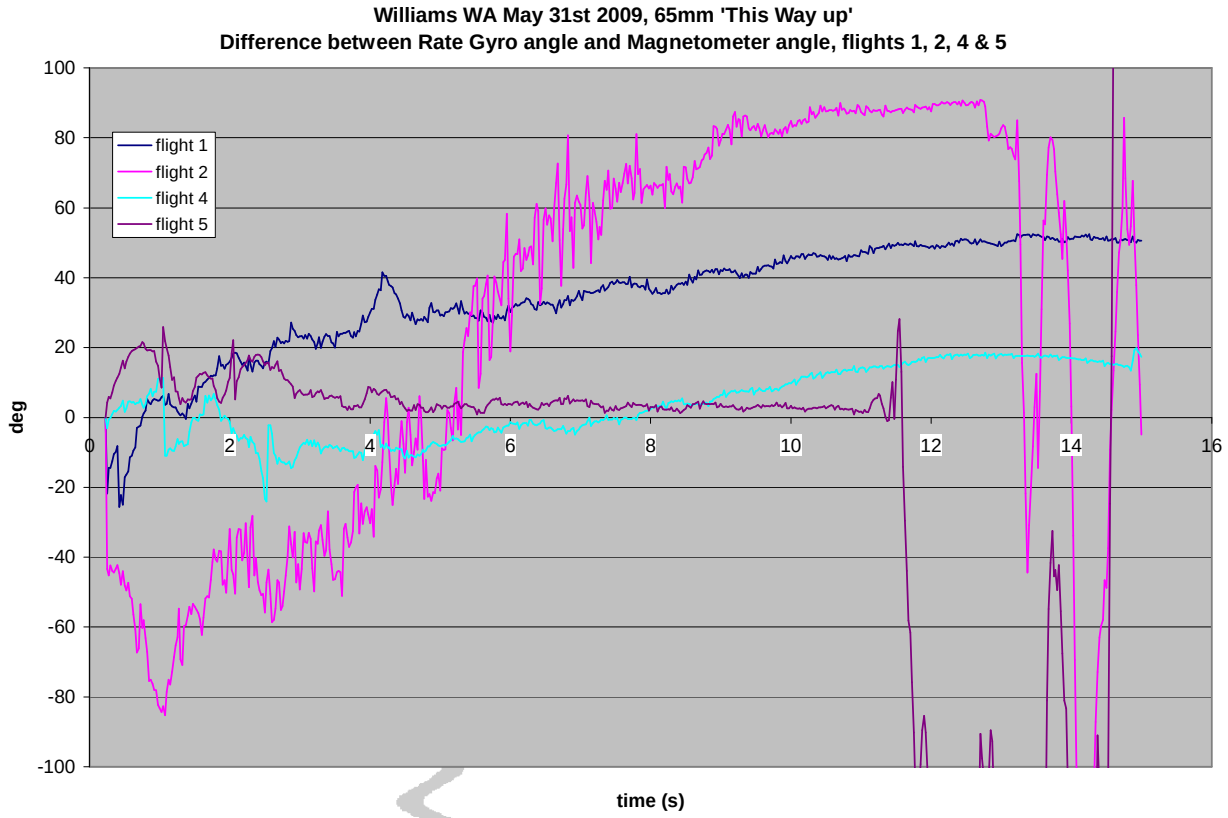

Figure 20 – Difference between gyro angle and Magnetometer angle

Figure 20 shows the difference in roll angle between integration of the rate gyro and the magnetometer. This difference is largest in flight 2, which is not as yet explained.

The differences for the other two flights is most likely to there not being any tilt compensation in this first version of the controller.

Other minor contributors to these errors are possibly due to the following :

- Rate gyro calibration error
- Rate gyro non-linearity
- Mechanical alignment error

5 Discussion

The first series of tests are very promising and very motivating.
The controller and actuators were able to maintain a closed loop roll angle error of $< \pm 30°$ for most of the duration of the 4 successful flights.
The data logging function, launch detection and servo supply worked as designed.

The gain schedule implemented seems to have achieved the target closed loop period of 1.0s, which is very pleasing. However, the actuator spent most of the flight in saturation due to a number of factors :

- Relatively high control loop stiffness for low airspeed
- Low damping factor realised
- Actuator phase lag

The system seems to be very poorly damped. However, without knowing how much phase lag exists in the servo actuator it is hard to say what affect the damping or velocity control gain has had.
However, to gain confidence in the accuracy and performance of the sensor systems, a more systematic and thorough calibration process is definitely required.

6 Further work

- Characterisation of servo actuator dynamic performance
- Calibration of rate gyro & integration process
- Calibration of magnetometer heading performance in vertical orientation
- Tilt compensation
- Attempt to resolve 'glitch' as seen in Test series 1, flight 2 at launch
- Gain schedule interpolation
- More flight testing with various gain schedules, including much longer closed loop period to eliminate effect of any actuator phase lag.
- Flights with on-board camera as absolute reference

Appendix 1 – Additional results from test series #1

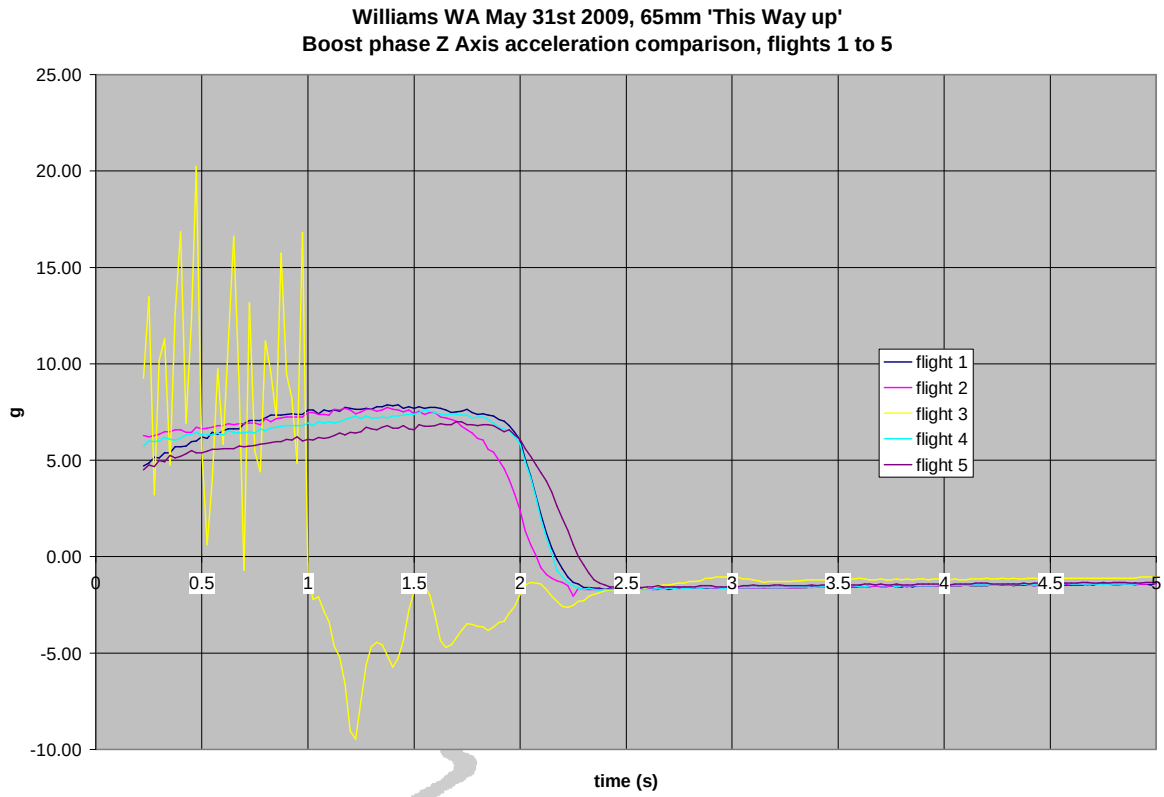

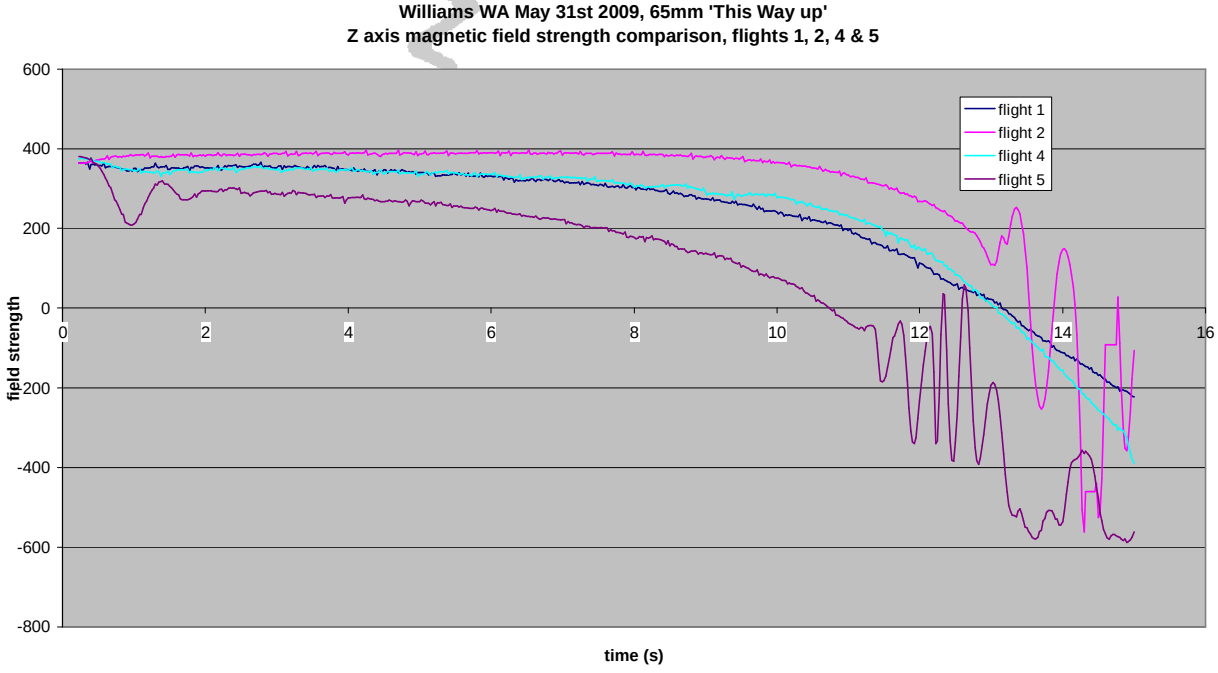

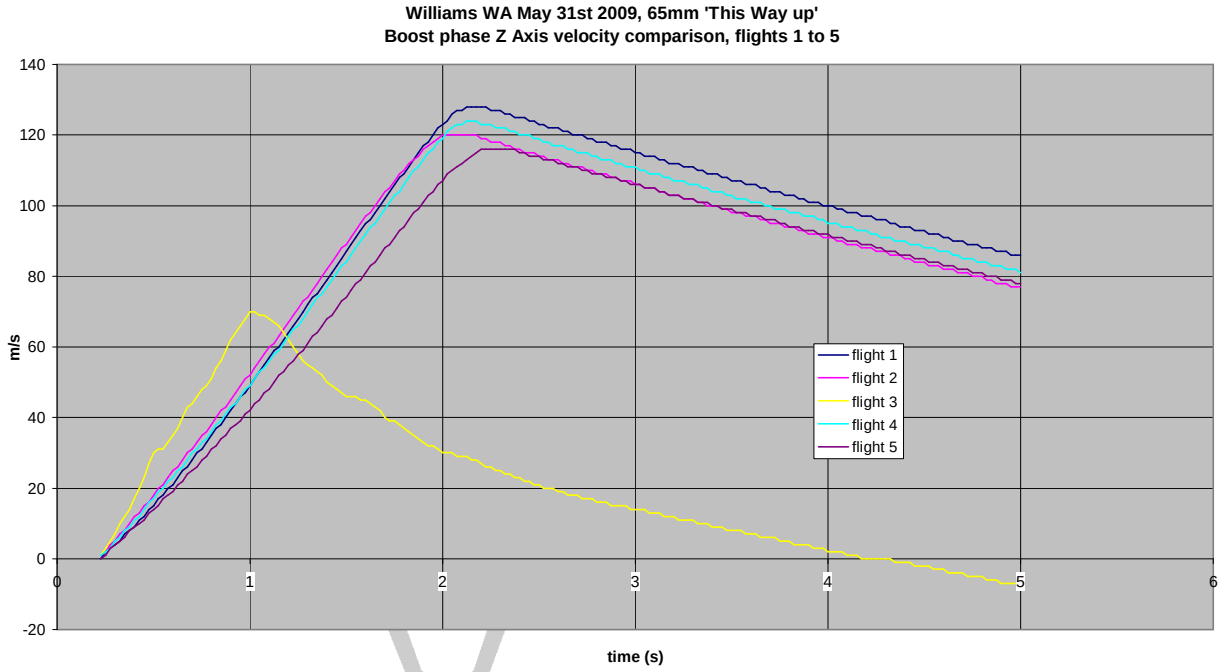

Appendix 2 – Various gain schedules for future flight testing

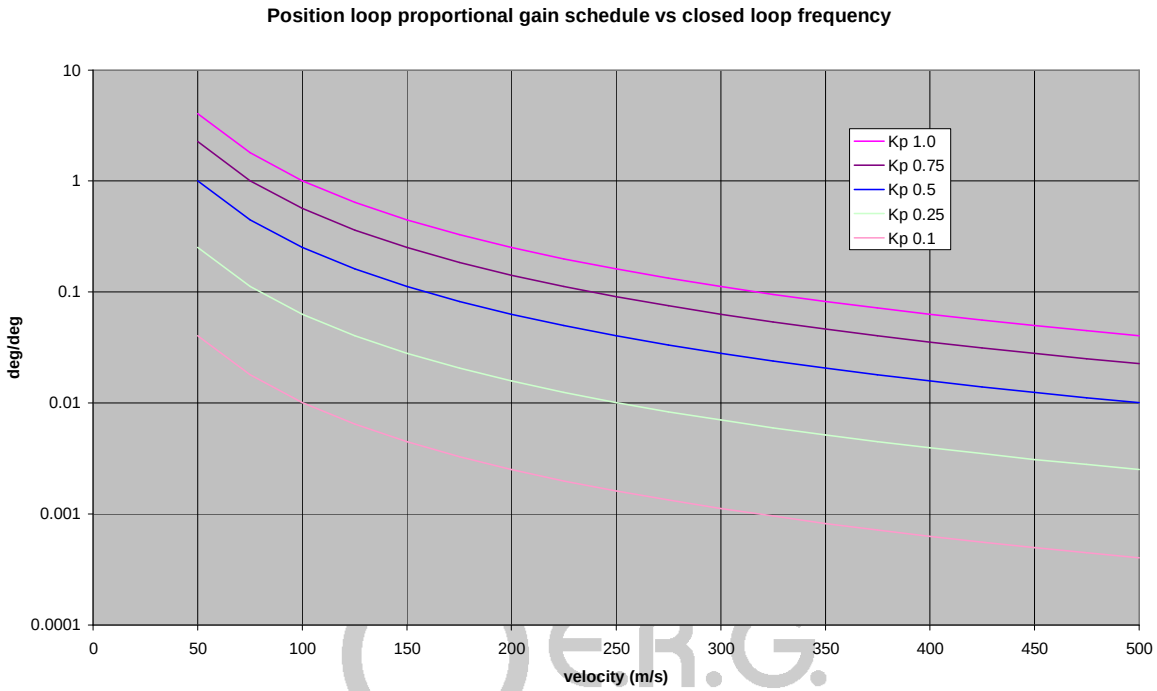

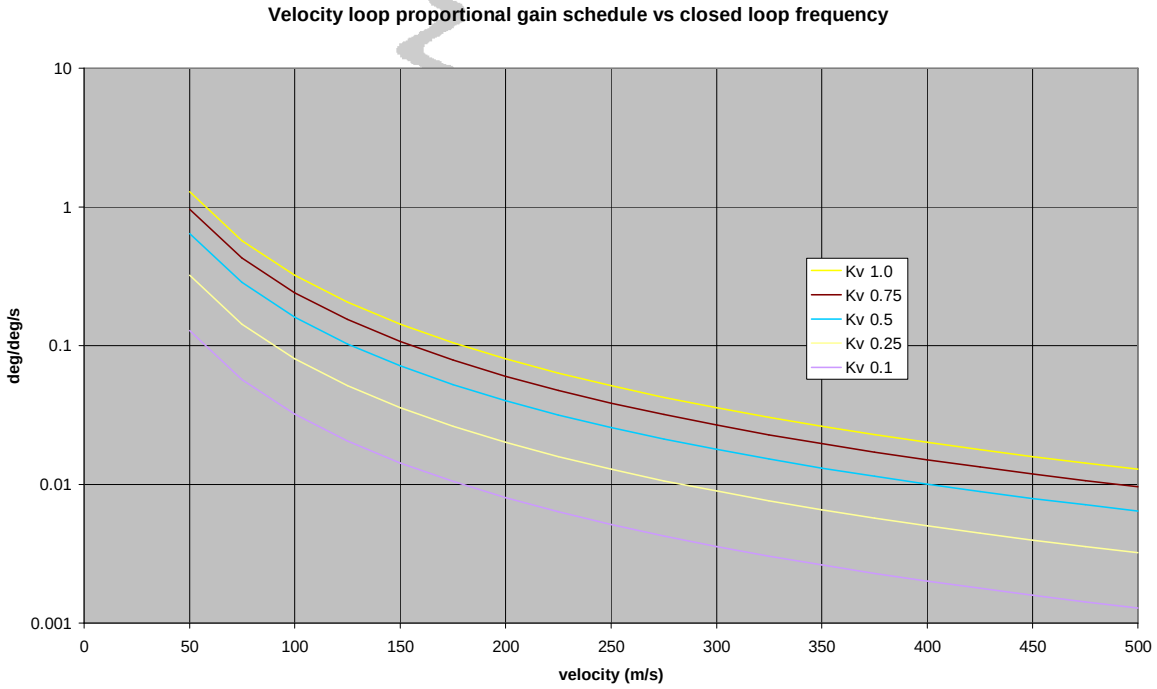

Appendix 3 - Gain schedules as used in microcontroller lookup table

Gain Schedule x 256, 38x38mm fin section

Freq	*Zeta*	**velocity m/s**	50	75	100	125	150	175	200	225	250	275	300	325	350	375	400	425	450	475	500
1	***1***	**Kp x 256**	1031	458	258	165	115	84	64	51	41	34	29	24	21	18	16	14	13	11	10
		Kv x 256	263	117	66	42	29	21	16	13	11	9	7	6	5	5	4	4	3	3	3
0.75	***1***	**Kp x 256**	580	258	145	93	64	47	36	29	23	19	16	14	12	10	9	8	7	6	6
		Kv x 256	246	109	62	39	27	20	15	12	10	8	7	6	5	4	4	3	3	3	2
0.5	***1***	**Kp x 256**	258	115	64	41	29	21	16	13	10	9	7	6	5	5	4	4	3	3	3
		Kv x 256	164	73	41	26	18	13	10	8	7	5	5	4	3	3	3	2	2	2	2
0.25	***1***	**Kp x 256**	64	29	16	10	7	5	4	3	3	2	2	2	1	1	1	1	1	1	1
		Kv x 256	82	36	21	13	9	7	5	4	3	3	2	2	2	1	1	1	1	1	1
0.1	***1***	**Kp x 256**	10	5	3	2	1	1	1	1	0	0	0	0	0	0	0	0	0	0	0
		Kv x 256	33	15	8	5	4	3	2	2	1	1	1	1	1	1	1	0	0	0	0

References

[1] Andrew Burns – assistance with aerodynamic simulation of specific fin sections